Int. Conf. on Ultra Wideband Systems and Technologies, pp. 280-284, November 2003, Reston, Virginia

ENERGY EFFICIENT METHODS OF INCREASING DATA RATE FOR ULTRA WIDEBAND (UWB) COMMUNICATIONS SYSTEMS

Nathaniel J. August, Woo Cheol Chung, and Dong Sam Ha

VTVT (Virginia Tech VLSI for Telecommunications) Laboratory,
Bradley Department of Electrical and Computer Engineering,
Virginia Tech, Blacksburg, VA 24061 – 0111, USA

Phone: 540-231-4942 Fax: 540-231-3362
E-mail: {nateaugu, wochung1, ha}@vt.edu
http://www.ee.vt.edu/~ha/

Abstract— **This paper investigates energy efficient methods of increasing data rate for *m*-ary pulse position modulation (PPM) of impulse-based ultra wideband (UWB) systems in a multipath environment. The data rate of *m*-ary PPM can be increased by decreasing the pulse repetition interval (PRI) and/or increasing the number of bits transmitted per symbol. However, increasing the data rate beyond a certain limit degrades energy efficiency in a multipath environment. We investigate the relationship between data rate and energy efficiency and seek suitable bounds on the number of bits per symbol and the PRI.**

Index Terms— **UWB, modulation, PRI, PPM, data rate, energy efficiency, multipath, interference**

I. INTRODUCTION

Ultra wideband (UWB) is not a new technology; however, it has gained great attention recently in industry as well as in academia. The wide bandwidth provides many advantages over narrowband such as high data rate, low probability of detection and intercept, robustness for multipaths, and low power dissipation. This paper explores energy efficient methods of increasing data rate for *m*-ary pulse position modulation (PPM), which is a commonly used modulation scheme for impulse-based UWB systems [1]-[5], [7], [8]. The data rate can be increased by decreasing the pulse repetition interval (PRI) and/or increasing the number of bits per symbol. However, these techniques may incur lower energy efficiency. We examine energy efficient methods to increase data rate in a multipath fading environment with additive white Gaussian noise (AWGN). In addition, we investigate a practical range of PRI values and number of bits per symbol in terms of energy efficiency.

II. PRELIMINARIES

FCC regulations define a UWB system as one with a fractional bandwidth of greater than 0.20 or an absolute bandwidth of greater than 500 MHz. The fractional bandwidth is the difference between the high and low corner frequencies at 10 dB attenuation. Since our work examines impulse-based systems, we consider the former definition. In addition to wide bandwidth, FCC regulations also require UWB systems to emit very low power, –41.3 dBm / MHz, over the spectrum from 3.1 GHz to 10.6 GHz. The low power requirements result in increased sensitivity of UWB signals to interference and fading.

A. UWB Pulse Shape

Gaussian monopulses and doublets are widely used for UWB systems owing to their desirable shapes of the spectrum and existence of simple closed form expressions [3], [4]. Figure 1 shows a Gaussian monopulse in the leftmost plot. The middle and rightmost plots show the pulse shape after bandpass filtering in the time domain and frequency domain. In our experiments, we used a filtered Gaussian monopulse with a spectrum that meets FCC regulations.

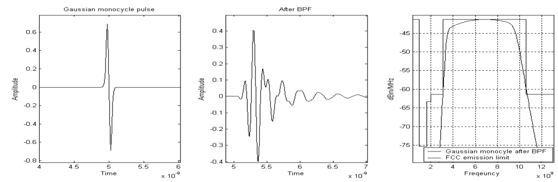

Figure 1: Gaussian Monopulse

B. UWB Modulation

Figure 2 shows a time domain representation of the binary PPM scheme. The transmitted train of Gaussian monopulses represents the data sequence "1001." The time period between two consecutive dotted vertical lines is the PRI, which determines the data rate for binary PPM. A pulse appearing before the reference point represents a binary '0', whereas a pulse after the reference point represents a binary '1'. Higher order *m*-ary extensions of PPM require *m* different non-overlapping pulse positions, i.e., *m* orthogonal basis functions, in this paper. Our investigation can readily be applied to time hopping multiple access [5], although it is somewhat orthogonal to our interests and not considered in this paper.

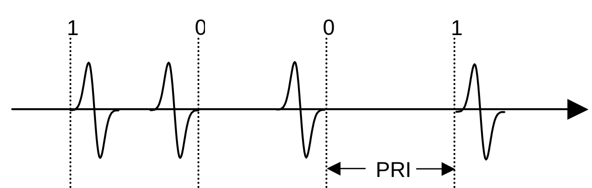

Figure 2: Pulse Position Modulation Scheme

Two types of interference are possible for PPM in this paper. Inter-symbol interference (ISI) is such that a delayed multipath from the previous symbol causes a decision error on the current symbol. In contrast, intra-symbol interference is such that a multipath of the current symbol provides a higher correlation than the first multipath, which causes misinterpretation of the current symbol. Obviously, ISI increases as PRI decreases, whereas intra-symbol interference increases as *m* increases.

In this paper, energy efficiency is defined in terms of the E_b/N_0 ratio required to achieve a target bit error rate (BER) as in (1).

$$EnergyEfficiency = \frac{BER_{target}^{-1}}{E_b/N_0} = \frac{1}{BER_{target} \cdot E_b/N_0} \quad (1)$$

Different *m*-ary modulation schemes are compared using (1) as the figure of metric. A modulation scheme is said to be more energy efficient than another modulation scheme if it achieves a target BER at a lower E_b/N_0.

III. UWB SYSTEM MODEL

A simulation model for our UWB system consists of three major parts: a transmitter, a channel, and a receiver, as shown in Figure 3. Note that channel coding achieves better performance in a practical system but is omitted in our model.

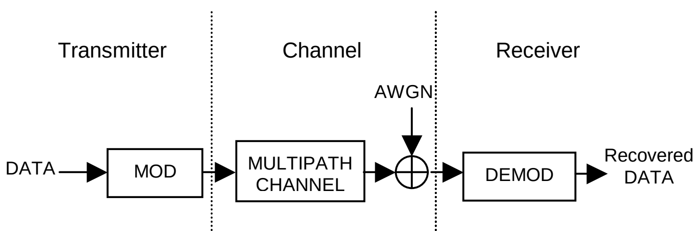

Figure 3: Block Diagram of UWB System Model

A. Transmitter Model

The transmitter modulates a bit stream (or parallel bit streams) into a train of output pulses. To simulate the output of a transmitter, we considered Gaussian monopulses with a center frequency of 6.85 GHz and a bandwidth of 10 GHz. Spectral energy outside the 3.1 GHz to 10.6 GHz range is attenuated with a bandpass filter and recovered with an equalizer at the receiver side. The output pulse train for PPM is described in (2).

$$\mathrm{PPM}_{\mathrm{TX}}(\mathrm{t}) = \sum_{\mathrm{j}=0}^{\mathrm{N}-1} \mathrm{p}(\mathrm{t} - j \cdot \mathrm{PRI} - n\mathrm{T}_{\mathrm{P}}) \quad (2)$$

The function p(t) is a Gaussian monocycle pulse, the parameter *n* specifies the modulation index, and T_P is the duration of a pulse. The PRI is the inverse of the symbol rate, and it ranges from 10 ns to 300 ns for our simulations.

B. Channel Model

The channel model considers the effects of multipath fading and AWGN. For multipath fading, we use Cassioli et al.'s indoor UWB channel model [6]. The model considers both large-scale and small-scale effects assuming omni-directional antennas. The time resolution is 2 ns, and one or more multipaths may arrive within this time period. The energy gain is updated every 2 ns after the first arriving path and is computed from both small-scale and large-scale effects. Due to the large-scale effects, this energy gain decays exponentially from the second arriving multipath to the last. The decay constant is a lognormal random variable with constant mean and variance. The small-scale effects consider the gain computed from the large-scale effects to be the mean of a stochastic variable with a gamma distribution.

Figure 4 displays the average power delay profile of Cassioli's model, which is useful to investigate the impact of PRI on performance. Time is measured relative to the first arriving multipath, and the amplitude of each vertical line represents the energy gain of each 2 ns delay bin. Note that a multipath "dies out" if its power is less than 6 dB above the noise floor in Cassioli's model, and all channel profiles "die out" within 300 ns. On average, over 92% of total energy arrives within 100 ns. This means that a PRI greater than 100 ns would experience very little ISI. Also note that between 15% of total energy for *m*=2 and 57% of total energy for *m*=32 may contribute to intra-symbol interference for a 1 ns pulse duration.

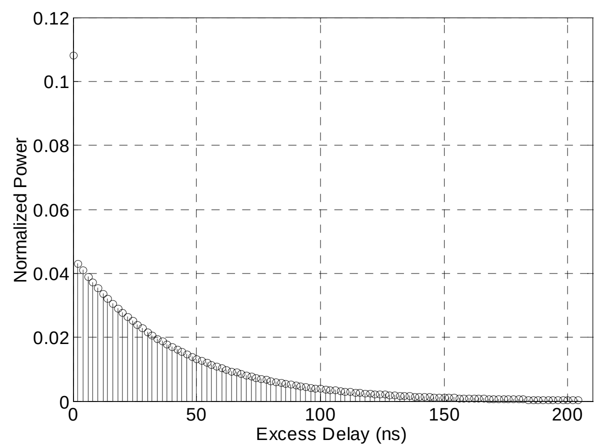

Figure 4: Average Power Delay Profile of the Channel

C. Receiver Model

The performance of a basic correlator receiver under multipath fading conditions is rather poor, since the total energy is spread over the multipaths. The first multipath contains relatively small energy compared with the total energy. We consider a perfect RAKE receiver (PRake) [7] to take advantage of the energy dispersed over the multipaths and to provide diversity. The PRake receiver employs maximal ratio combining (MRC), which considers the energy of each multipath scaled by the gain. Note that some multipaths will encounter more ISI and intra-symbol interference than others. Any narrowband interference from the received signal is filtered out before being received by the PRake receiver.

IV. Simulation Results

We modeled the UWB system in ADS (Advanced Design System) and simulated to investigate the effect of both PRI and the number of bits per symbol on data rate and energy efficiency in terms of BER versus E_b/N_0. The simulation considers one to five bits per symbol; hence the values of *m* are 2, 4, 8, 16, and 32. The PRI ranges from 10 ns to 300 ns in increments of 10 ns. Since the step of the modulation index is set to 1 ns for our simulation, *m*-ary PPM modulation requires at least *m* ns guard time to prevent overlap of frames. Thus, *m*=16 was not simulated for a PRI of 10 ns, and *m*=32 was not simulated for PRIs of 10 ns, 20 ns, and 30 ns.

A system configuration represents the combination of one possible value of PRI with one possible value of *m*. We simulated all possible configurations with E_b/N_0 ranging from -10 dB to 15 dB. To avoid excessive simulation time, we limited the minimum BER to 10^{-3}, if a BER of 10^{-3} is attainable for the configuration. We simulated each E_b/N_0 point until the simulator encountered an estimation relative variance of less than 0.01 in each bit stream. Since the channel model varies due to small-scale effects, we obtained performance trends by averaging the results over 100 instances of the channel model. Note that averaging mitigates such phenomena as unbalanced BER [8].

To ensure correctness of our models, we first compared the simulated BER vs. E_b/N_0 in AWGN with theoretical results [9], and we confirmed that our results matched the theoretical ones. Next, we introduced the multipath channel, which disperses energy over time and introduces both inter-symbol and intra-symbol interference.

A. Effect of m on Energy Efficiency

For E_b/N_0 less than 5dB, we observed that AWGN, rather than multipath interference, is the major source of bit errors. Thus the simulation results match the theoretical performance predicted for AWGN. Note that for low values of E_b/N_0, there is no advantage in energy efficiency for a larger number of bits per symbol in AWGN.

Figure 5 (a) shows the effects of varying *m*, i.e., the number of bits per symbol, for an E_b/N_0 of 5 dB. The graph also displays the theoretical performance under AWGN. As expected, the BER performance becomes worse for the multipath environment as the PRI shortens, while the performance is independent of the PRI under AWGN. As *m* increases, the BER performance improves monotonically for the AWGN. Under the multipath environment, the BER improves slightly between *m*=2 and *m*=4, except at the short PRIs of 10 ns and 20 ns. Beyond *m*=4, the BER degrades slightly in the multipath environment. This is because intra-symbol interference offsets the benefit of a larger *m*, i.e., a larger orthogonal signal set.

When E_b/N_0 increases from 5dB to 10 dB, as shown in Figure 5 (b), the BER performance improves for every PRI and for every *m*. The performance improvement is more significant, in general, for a smaller *m* and a larger PRI. For example, the BER improves by a factor of 26 for *m*=2 and PRI=300 ns, while it only improves by a factor of 8 for *m*=16 for the same PRI. This implies that ISI and intra-symbol interference are a less dominant source of error than noise for a smaller *m*.

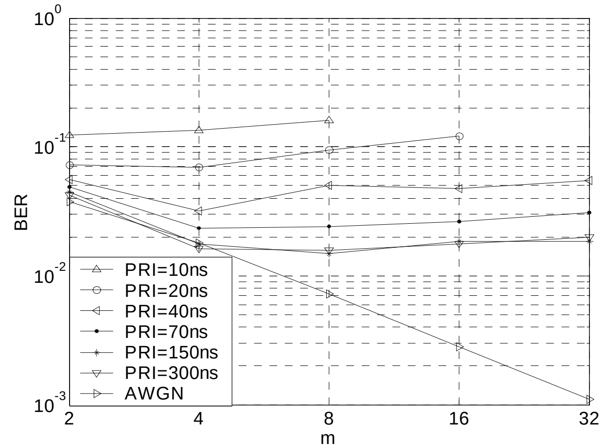

(a) E_b/N_0 = 5 dB

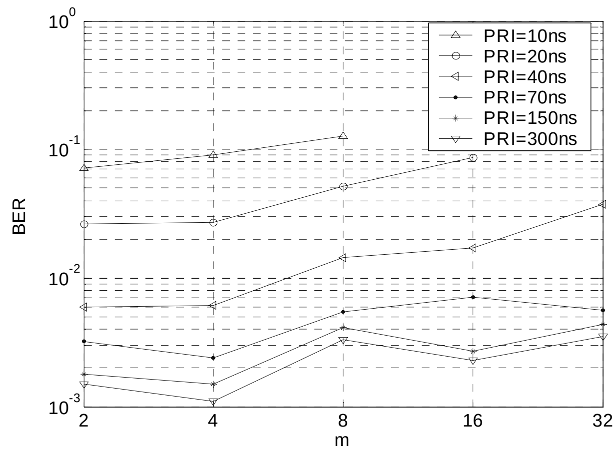

(b) E_b/N_0 = 10 dB

Figure 5: BER Performance for Various *m*

We note that increasing the number of bits per symbol increases both energy efficiency and data rate in AWGN. However, as *m* increases beyond 4 in the multipath channel, performance degradation of the intra-symbol interference offsets the performance increase from the orthogonal symbol set. However, the overall degradation is slight, so it is still advantageous to use a larger number of bits per symbol to achieve a high data rate.

B. Effect of PRI on Energy Efficiency

Another approach to increase the data rate is to decrease the PRI. Figure 6 shows PRI versus BER for E_b/N_0 of 5 dB and 10 dB. Each *m*-ary modulation shows rapid degradation in performance below a certain region of PRI values. For example, if the PRI changes from 40 ns to 30 ns for *m*=2, the BER increases by a factor of 2.6 in Figure 6 (b). Likewise, if the PRI changes from 70 ns to 60 ns for *m*=32, the BER increases by a factor of 2.4. ISI increases rapidly as PRIs decrease below a certain region, hence the rapid performance degradation. The region of PRI values where performance starts to degrade

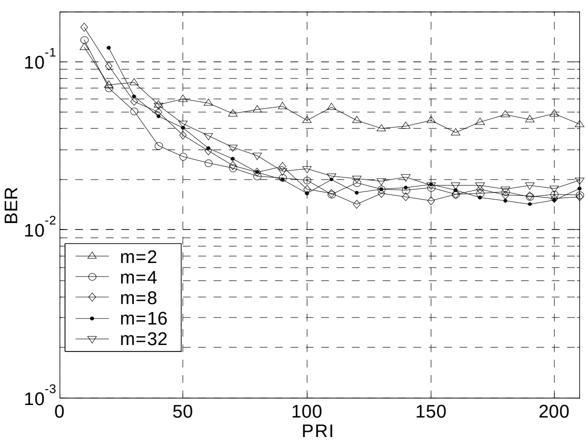

(a) E_b/N_0 = 5 dB

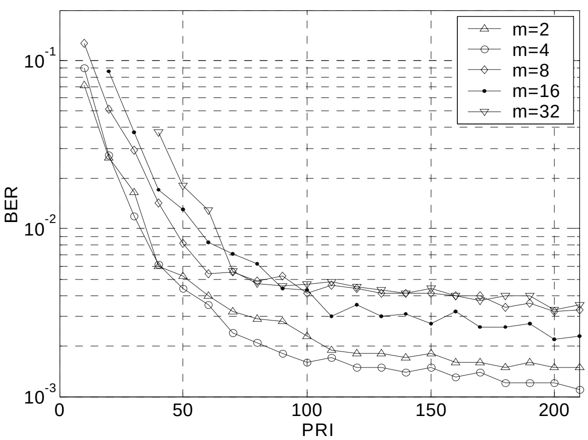

(b) E_b/N_0 = 10 dB

Figure 6: BER Performance for Various PRIs

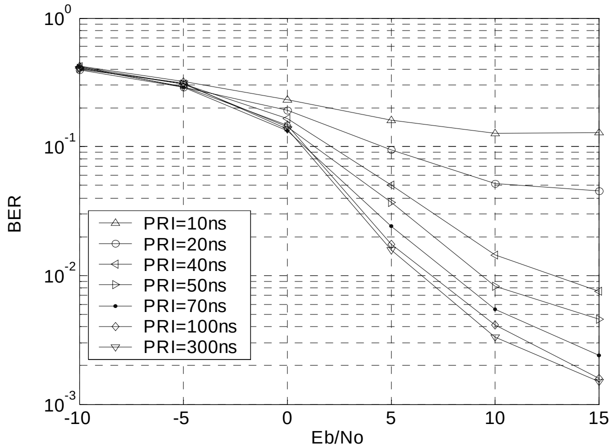

Figure 7: BER versus E_b/N_0 for various PRIs under *m*=8

TABLE I
RECOMMENDED MINIMUM AND MAXIMUM PRI

M	Max. PRI (ns)	Data Rate (Mbps)	E_b/N_0 for BER=10^{-2}	Min. PRI (ns)	Data Rate (Mbps)	E_b/N_0 for BER=10^{-2}
2	100	10.0	7.5 dB	40	25.0	8.9 dB
4	100	20.0	6.6 dB	40	50.0	8.6 dB
8	100	30.0	6.9 dB	50	60.0	9.3 dB
16	110	36.4	6.9 dB	60	66.7	9.3 dB
32	120	41.6	6.9 dB	70	71.4	8.5 dB

includes longer PRI values for higher *m* because *m*-ary PPM modulation allows symbol positions from the start of the frame to $m*T_P$ ns after the start of the frame. Thus, to encounter similar levels of ISI, 32-ary modulation requires 30 ns longer guard time than binary modulation. For example, 45% of total energy arrives later than 30 ns after the first path in Figure 4, and these multipaths contribute ISI for a PRI less than $(30 + m*T_P)$ ns.

Increasing the PRI beyond a certain region does little to improve efficiency and reduces the data rate. In Figure 4, multipaths completely "die out" after 204 ns and only 7.5% of energy arrives later then 100 ns after the first path. Thus, there is little benefit to set the PRI greater than $(100 + m*T_P)$ ns.

As is evident from Figure 6, increase of E_b/N_0 from 5 dB to 10 dB improves BER performance for all system configurations. Figure 7 examines this performance improvement more closely for *m*=8. Higher E_b/N_0 improves the BER performance more significantly for longer PRIs. For short PRIs of 10 ns or 20 ns, Figure 7 shows that BER improvement saturates and causes an error floor at around E_b/N_0=10 dB. For short PRIs, the combination of ISI and intra-symbol interference dominates the errors caused by noise at relatively low E_b/N_0. For longer PRIs, there is much less ISI, and intra-symbol interference does not dominate the noise and cause an error floor until higher E_b/N_0.

C. Bounds for PRI and m

Close examination of Figure 7 suggests that there is a desirable region of PRI values for a given *m* and a target BER. This range is bounded by the *min_PRI* and the *max_PRI*.

Increasing the PRI beyond the *max_PRI* results in little improvement in energy efficiency at the cost of a lower data rate. In this paper, we consider the *max_PRI* to be the minimum PRI that attains a BER of 10^{-2} with an E_b/N_0 within 1 dB of a 300 ns PRI. Decreasing the PRI below the *min_PRI* results in poor energy efficiency. In this paper, we consider the *min_PRI* to be the minimum PRI that attains a BER of 10^{-2} with an E_b/N_0 within 3 dB of the *max_PRI*.

For example, Figure 7 shows that for *m*=8, the *max_PRI* is around 100 ns and the *min_PRI* is around 50 ns. Due to space limitations, graphs are not shown for the other *m*-ary cases. Table I summarizes the *min_PRI* and *max_PRI* values for each *m*-ary PPM under the multipath environment. The first column lists values of *m*, the second column presents the *max_PRI*, the third column displays the resulting data rates (computed from *m* and the PRI), and the fourth column lists the required E_b/N_0 for the given *m* and PRI to achieve a target BER of 10^{-2}. The next three columns present results for the *min_PRI* values.

As shown in the columns of E_b/N_0, PPM maintains similar energy efficiency for a BER of 10^{-2} for all values of *m* in the table with a PRI between *min_PRI* and *max_PRI*. However, Table I shows that increasing the number of bits per symbol starts to show limited improvement in data rate for *m* greater than 16. This is because *m* increases exponentially as the number of bits per symbol increases linearly. As a result the minimum guard time between symbols - and hence the PRI - increases rapidly. In fact, data rate fails to increase beyond five bits per symbol (*m*=32). For example, 128-ary PPM requires a guard time of at least 128 ns in AWGN for T_P = 1ns, which results in a maximum data rate of about 54 Mbps. 32-ary PPM can achieve a maximum data rate of over 156 Mbps in AWGN and, as shown in Table 1, 71.4 Mbps considering multipaths.

Table I shows that the configuration with *m*=32 and PRI=70 achieves the maximum data rate of 71.4 Mbps. Note that this is more than a seven-fold increase in data rate from the case of *m*=2 and PRI=100 ns. This improvement in data rate is achieved with only 1 dB penalty in energy efficiency. Note, however, that there are other penalties. Moving from top to bottom (increasing *m*) in Table I increases receiver complexity. Additionally, moving from the top left (low *m*, long PRI) of the table to the bottom right (high *m*, short PRI) increases radiated power. If circuit complexity is a concern, the number of bits per symbol may be reduced with no penalty in efficiency. If radiated power is a concern, the number of bits per symbol may be reduced and/or the PRI may be increased.

V. CONCLUSION

In this paper, we investigated efficient methods to increase data rate for an *m*-ary PPM impulse-based UWB communications system under multipath fading. As we increase the data rate -- either by increasing the number of bits per symbol or by decreasing the PRI -- inter-symbol and intra-symbol interference degrades the BER performance. We suggested minimum and maximum PRI values for each type of *m*-ary PPM. Further decreases in PRI beyond the minimum result in inefficient performance, whereas further increases beyond the maximum PRI result in limited efficiency gains at the expense of data rate. We also suggested a maximum number of 5 bits per symbol. For more than 5 bits per symbol, the exponential increase in guard time reduces the data rate even though there are more bits per symbol.

Higher E_b/N_0 improves performance more significantly, in general, for a smaller *m* and a larger PRI. This means that configurations with larger *m* and shorter PRI are more susceptible to ISI and intra-symbol interference. However, at large E_b/N_0, intra-symbol interference dominates all other sources of distortion, and an error floor appears for all system configurations.

Although it is possible to efficiently increase data rate, there exist tradeoffs between data rate, radiated power, and receiver complexity. Reducing the number of bits per symbol decreases both radiated power and receiver complexity, while increasing the PRI reduces radiated power. Careful selection of both PRI and the number of bits per symbol is required to meet constraints on energy efficiency, radiated power, and data rate.

Finally, we note that these results are independent of the exact pulse shape, as simulations with Gaussian doublets provided similar trends. This indicates that system performance is more dependant upon the signal constellation and the multipath model than the exact type of pulse shape, as long as the pulse shape is such that multipaths can be resolved for the given channel model.

REFERENCES

[1] R.A. Scholtz and M.Z. Win, “Impulse radio,” IEEE PIMRC’97, 1997.

[2] M.L. Welborn, “System considerations for ultra-wideband wireless networks,” *Proceedings of IEEE Radio and Wireless Conference (RAWCON) 2001*, pp.5-8, 2001.

[3] X. Chen and S. Kiaei, "Monocycle shapes for ultra wideband system" *Proceedings of the 2002 IEEE International Symposium on Circuits and Systems (ISCAS 2002)*, vol.1, pp.I597-I600, 2002.

[4] L. Zhao and A.M. Haimovich, “Capacity of m-ary PPM ultra wideband communications over AWGN channels,” *IEEE Vehicular Technology Conference*, vol. 2, pp1191-1195, Oct. 2001.

[5] F.R-Mireles and R.A. Scholtz, "Multiple access with time hopping and block waveform PPM modulation," *IEEE ICC '98*, June 1998.

[6] D. Cassioli, M.Z. Win, and A.F. Molisch, “The ultra-wide bandwidth indoor channel: from statistical model to simulations,” *IEEE Journal on Selected Areas in Communications*, Vol. 20, No. 6, pp. 1247-1257, August 2002.

[7] F.R-Mireless and R.A. Scholtz, “Peformance of equicorrelated ultra-wideband pulse-position-modulated signals in the indoor wireless impulse radio channel,” *1997 IEEE Pacific Rim Conference on Communications, Computers, and Signal Processing*, vol.2, pp. 20-22, Aug. 1997

[8] L. Ge, G. Yue, and S. Affes, “On the BER peformance of pulse position modulation UWB radio in multipath channels,” *Digest of Papers. 2002 IEEE Conference on Ultra Wideband Systems and Technologies*, pp 231-234, May 2002.

[9] J.G. Proakis, *Digital Communications*, McGraw-Hill Inc., 1995.